

Exceptional Point of Sixth Order Degeneracy in a Modified Coupled Resonators Optical Waveguide

Mohamed Y. Nada and Filippo Capolino

Department of Electrical Engineering and Computer Science, University of California, Irvine, CA 92697, USA

We demonstrate for the first time the occurrence of a sixth order exceptional point of degeneracy (EPD) in a multimode optical photonic structure by using a modified periodic coupled resonators optical waveguide (CROW), at the optical wavelength $\lambda_e = 1550\text{nm}$. The 6th order EPD is obtained in a CROW without the need of loss or gain. Such EPD corresponds to a very special band edge of the periodic photonic structure where six eigenmode coalesce, so we refer to it as the 6th order degenerate band edge (6DBE). The quality factor Q of an optical cavity made of such a periodic waveguide operating near the 6DBE shows exceptional scaling with the structure length as $Q \propto N^7$ with N being the number of unit cells in the periodic finite structure. Furthermore, we elaborate on two applications of the 6DBE: ultra-low-threshold lasers, with threshold that scales as N^{-7} , and highly sensitive sensors. The proposed 6DBE-CROW may also find applications in modulators, optical switches, nonlinear devices, and Q -switching cavities.

I. Introduction

An exceptional point of degeneracy (EPD) is a point at which two or more system eigenmodes coalesce in both eigenvalues and eigenvectors [1]–[4]. In this paper we focus on an EPD of sixth order in a lossless and gainless structure, where the order of the EPD is determined by the number of coalescing eigenmodes at the exceptional point. EPDs in lossless structures [5]–[10] are associated with slow-wave phenomena, including band edges, whereby the group velocity of the propagating wave is almost vanishing [11], [12]. In the optical realm, slow-wave phenomenon has invaded many intriguing aspects of optical resonators in which nonlinearities [13], and gain/absorption [14], among other features, can be significantly enhanced. Generally, the existence of an EPD in electromagnetic systems leads to unique properties that cannot be obtained in conventional structures such as the giant field enhancement, strong enhancement in the local density of states [9], unconventional scaling of the quality factor (Q factor) with structure length [8]–[10], [15], and extreme sensitivity to perturbations [16], [17]. Such properties can be utilized in various applications like modulators, switches, high quality factor resonators and sensors.

Optical sensors based on the confinement of light in optical microresonators (or microcavities) have received a surge of interest nowadays [18], [19]. Sensors based on slow light in optical microcavities [20] require the usage of high Q factor resonators [21], [22], which can be done by designing the optical resonators to operate near an EPD [10]. High Q resonators are also beneficial for other different applications including filters [23], optical switching [24], optical delay line devices [25], and lasers [26]. On the other hand, cascading a chain of coupled micro resonators, as shown in [27], has stimulated a great interest in studying coupled resonator optical waveguides (CROWs) as special devices for slow light transport [25], [4].

We stress that the EPD presented in this paper is obtained in periodic structures without the existence of loss or gain in the system. The simplest EPD is the one that exists at the band edge

of any periodic structure due to the coalescing of two eigenmodes. Such 2nd order EPD is referred to as the regular band edge (RBE) [5]. The 3rd order EPD was found in non-reciprocal structures [3], [28] and it is often referred to as the stationary inflection point (SIP). Recently the SIP has been shown in lossless, reciprocal structures such as a 3-way waveguide [29] and the modified CROW [4]. The 4th order EPD is a band edge of a periodic structure, so we refer to it as the degenerate band edge (DBE). Such an EPD was explored in various structures [5], [8], [9], [30] and it was even found in CROWs [4], [10]. Higher orders EPDs were studied theoretically in [7] assuming idealistic coupled mode theory without referring to any particular structure, and to the best of our knowledge, EPDs of high orders (greater than 4) have not been found in any realistic optical structure yet.

In this paper, we show for the first time an optical structure made of a CROW side-coupled to a rectangular waveguide that is capable of exhibiting a 6th order EPD in its dispersion diagram. Throughout the paper we refer to this 6th order EPD as 6DBE since it is obtained at the band edge of the CROW without the need of loss or gain. We also show some of the unique properties of CROWs operating near the 6DBE such as the scaling of the quality factor with cavity length. Finally, we explore two interesting applications of CROW structures operating in close proximity to the 6DBE: low threshold laser and ultra-sensitive sensors.

II. CROW with 6th Order EPD

We introduce the modified coupled resonator optical waveguide (CROW) structure shown in Fig. 1(a) which is capable of exhibiting various orders of EPDs. This structure represents a three-way waveguide, i.e., there are three propagating or evanescent modes in each positive and negative z -direction. The theory of EPDs in CROWs was discussed in [4], where we have discussed degeneracies of orders 2,3 and 4. In this paper we show the first realization of a waveguide that exhibits a 6th order EPD in its dispersion diagram, which is the maximum degeneracy order with a three-way waveguide. The structure is made of a chain of

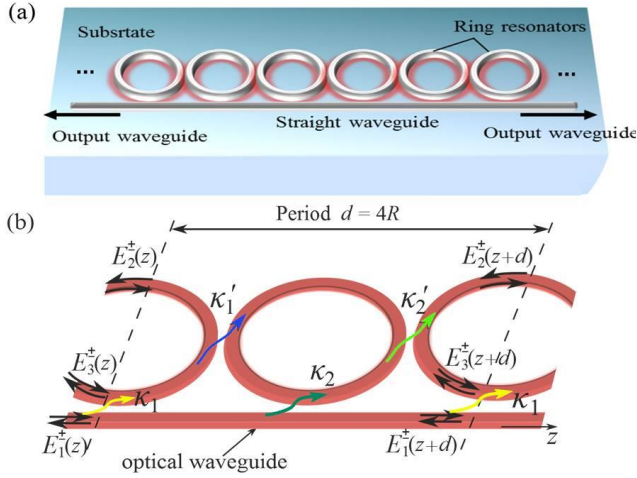


FIG. 1. (a) The 6DBE-CROW consists of a chain of coupled ring resonators of radius R that is side coupled to a rectangular straight waveguide. The 6DBE-CROW is periodic in the z -direction with a period $d = 4R$. (b) A unit cell of the periodic 6DBE-CROW with the electric field wave amplitudes defined at the periodic-cell boundaries. The field coupling coefficients between the coupled rings are alternating between κ_1' and κ_2' whereas the field coupling coefficients between the straight optical waveguide and the rings are alternating between κ_1 and κ_2 .

coupled ring resonator optical waveguides where the field coupling coefficients are alternating from one ring to another as κ_1' and κ_2' , and the outer radius of each ring is R . The CROW is side-coupled to a uniform optical waveguide with alternating field coupling coefficients κ_1 and κ_2 as shown in Fig. 1. We call this modified CROW, designed to exhibit the 6th order EPD, as 6DBE-CROW.

Following [4], we assume that the eigenwaves' phase propagation in the positive/negative z -direction of the waveguides and the rings is represented by $e^{\pm in_w k_0 z}$ and $e^{\pm in_r k_0 z}$, respectively, where n_w, n_r are the effective refractive indices of the waveguide and the rings and $k_0 = \omega/c$ is the wavenumber in free space. Also, throughout the paper we assume that the time convention is $e^{-i\omega t}$. Each ring resonator external radius is R so that the 6DBE-CROW is periodic with a period $d = 4R$ (the unit cell consists of 2 rings), where for simplicity we neglect the gap dimensions between adjacent rings as was done in [4], [10], [11].

To explore the unique modal characteristics of this 6DBE-CROW, we represent the wave propagation along z using complex electric field wave amplitudes that are defined as shown in Fig. 1(b). Therefore, at any point z , there are three complex electric field wave amplitudes that propagate in the positive z -direction described by the 3-dimensional vector $\mathbf{E}^+(z) = [E_1^+(z), E_2^+(z), E_3^+(z)]^T$ and another three field wave amplitudes that propagate in the negative z -direction represented by the vector $\mathbf{E}^-(z) = [E_1^-(z), E_2^-(z), E_3^-(z)]^T$. We define a state vector composed of the six field amplitude components as

$$\boldsymbol{\Psi}(z) = \begin{bmatrix} \mathbf{E}^+(z) \\ \mathbf{E}^-(z) \end{bmatrix} \quad (1)$$

Using the coupled mode theory [4], [11], [31] the evolution from cell to cell of the state vector is governed by the equation $\boldsymbol{\Psi}(z+d) = \mathbf{T}\boldsymbol{\Psi}(z)$, where d is the period, and \mathbf{T} is a 6×6 transfer matrix representing the evolution across a unit cell and the expression of \mathbf{T} is given in Appendix A in [4]. We utilize this transfer matrix formalism to investigate the evolution of the state vector along the 6DBE-CROW hence we derive the eigenwave characteristics. We obtain the $\omega-k$ dispersion relation of the 6DBE-CROW eigenmodes as

$$D(k, \omega) \equiv \det[\mathbf{T} - \zeta \mathbf{1}] = 0; \quad D(k, \omega) = \sum_{l=0}^6 c_l(\omega) \zeta^l \quad (2)$$

where $\zeta = \exp(ikd)$, k is the Bloch wavenumber along z , ω is the angular frequency, and $\mathbf{1}$ is the 6×6 identity matrix. The polynomial coefficients $c_l(\omega)$ are function of frequency and the 6DBE-CROW parameters. It is clear from the dispersion relation (2) that at any frequency, there exist six Bloch eigenmodes guided by the 6DBE-CROW and we showed in [4] that there are particular frequencies at which some eigenmodes coalesce in both their wavenumber and eigenvectors. The number of coalescing eigenwaves at the EPD represents the order of the EPD. In [4] we have shown different designs where the proposed CROW can support 2nd, 3rd and 4th order EPDs. However, in this paper we show that such CROW can exhibit also a 6th order EPD in its dispersion diagram, which is the highest order that can be obtained using such structure. When such a condition occurs, the six eigenvectors of \mathbf{T} coalesce as discussed in the next section. It is important to point out that this is the first time where the 6th order EPD is shown in an optical realistic structure.

III. Mathematical Description of The Sixth Order EPD

When an electromagnetic system exhibits a sixth order EPD in its dispersion diagram, exactly at the EPD frequency the unit-cell transfer matrix \mathbf{T}_e contains six degenerate eigenvalues ζ_e , where the e subscript denotes the EPD. There are six degenerate eigenvectors, therefore the algebraic multiplicity of ζ_e is 6 but its geometrical multiplicity is 1. Hence, the T-matrix \mathbf{T}_e is similar to a Jordan matrix of order 6 which is represented as

$$\mathbf{T}_e = \mathbf{V} \mathbf{\Lambda}_e \mathbf{V}^{-1}, \quad \mathbf{\Lambda}_e = \begin{pmatrix} \zeta_e & 1 & 0 & 0 & 0 & 0 \\ 0 & \zeta_e & 1 & 0 & 0 & 0 \\ 0 & 0 & \zeta_e & 1 & 0 & 0 \\ 0 & 0 & 0 & \zeta_e & 1 & 0 \\ 0 & 0 & 0 & 0 & \zeta_e & 1 \\ 0 & 0 & 0 & 0 & 0 & \zeta_e \end{pmatrix} \quad (3)$$

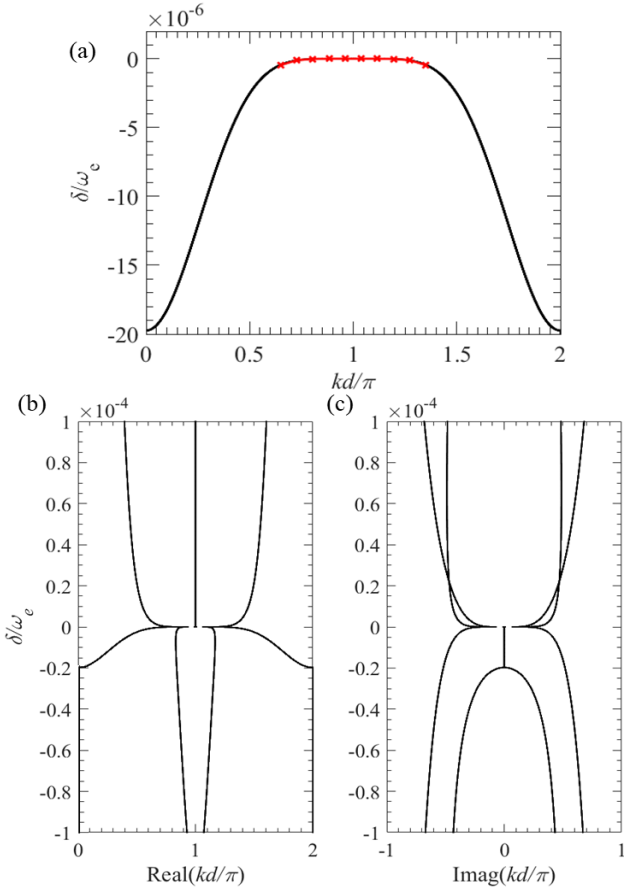


FIG. 2. Floquet-Bloch wavenumber dispersion diagram of the 6DBE-CROW whose unit cell is shown in Fig. 1(b). (a) Only the propagating modes with purely real wavenumber values are shown, where the 6DBE occurs at the frequency corresponding to the wavelength $\lambda_e = 1550\text{nm}$ and $\delta = \omega - \omega_e$. The red cross markers show the dispersion fitting formula given by equation (5) with the fitting flatness parameter $\eta_e = 0.00025$. (b) Complex dispersion diagram showing both real and imaginary parts of the six Floquet-Bloch wavenumbers k versus normalized real frequency δ/ω_e . This diagram shows six wavenumbers coalescing at $\omega = \omega_e$. The parameters of the unit cell are chosen as the radius is $R = 13\mu\text{m}$, the cross coupling coefficients are $\kappa_1 = 0.89$, $\kappa'_1 = 0.03$, $\kappa_2 = 0.4$, $\kappa'_2 = 0.72$, and the effective refractive indices are $n_r = 2.45$, and $n_w = 2.5$.

Here $\underline{\mathbf{V}}$ is the similarity transformation matrix whose columns comprise one regular eigenvector and five generalized eigenvectors corresponding to the six degenerate eigenvalue solutions $\zeta_e = \exp(ik_e d)$ where k_e is the wavenumber at the 6DBE and $\underline{\mathbf{\Lambda}}_e$ is a 6×6 Jordan block.

Due to reciprocity, the six Bloch wavenumber solutions of (2) have to form pairs made of negative and positive values, i.e., k and $-k$ are both solutions. Since there are only six solutions, the 6DBE has to be at k_e and $-k_e$ simultaneously, i.e., $k_e = -k_e$, which leads to only two possibilities for the k_e value: either $k_e = 0$ or $k_e = \pi/d$, i.e., either at the edge or center of the first Brillouin

zone (BZ), respectively (defined here by the interval $[0 \ 2\pi/d]$). In other words, this sixth order EPD cannot occur at any other point of the BZ in this reciprocal system. This follows that the dispersion relation (2), when fixing the frequency exactly at the 6DBE one, must be in the form

$$(\zeta \pm 1)^6 = 0 \quad (4)$$

where the + sign corresponds to the case when $k_e = 0$ and the - sign corresponds to the case when $k_e = \pi/d$; which is the case discussed next.

There are many possible points in the parameter space of the 6DBE-CROW to realize the 6DBE that can be obtained by proper tuning of the coupling parameters, effective refractive indices and radius of the rings. To facilitate the tuning of the design parameters, we equate the coefficients of the polynomial (2) at the desired 6DBE frequency to those of (4). Hence, we can find a set of necessary equations governing the choice of the different 6DBE-CROW parameters that can be solved numerically to determine the different parameters. Note that equating the coefficients of the polynomials (2) and (4) at a specific desired optical frequency provides a necessary condition to find the 6DBE at that desired frequency, but the sufficient condition for the 6DBE to exist is to check that the system six eigenvectors are coalescing at such desired 6DBE frequency.

In all the subsequent analysis and results, the 6DBE wavelength is designed to be at the optical wavelength $\lambda_e = 2\pi c/\omega_e = 1550\text{nm}$ where ω_e is the 6DBE angular frequency. We have solved the necessary equations and found the 6DBE-CROW parameters that may lead to the existence of the 6DBE and we have confirmed the existence of the 6DBE by the coalescence of the six eigenvectors. The parameters of the unit cell are as follows: radius is $R = 13\mu\text{m}$, the cross coupling coefficients

are $\kappa_1 = 0.89$, $\kappa'_1 = 0.03$, $\kappa_2 = 0.4$, $\kappa'_2 = 0.72$, and the effective refractive indices are $n_r = 2.45$, and $n_w = 2.5$. Note that the width and thickness of the waveguides are neglected here but they must be designed to allow the propagation of a single fundamental mode and to achieve the designed coupling parameters and effective refractive indices. The dispersion diagram of this unit cell is shown in Fig. 2, where in Fig. 2(a) we show only the propagating modes, i.e., modes with zero imaginary part of the Bloch wavenumber k , while in Fig. 2(b) we show the complete complex dispersion diagram in order to see clearly the coalescence of the six modes at the EPD. In the dispersion diagram in Fig. 2 the 6DBE point is characterized by ω_e and $k_e = \pi/d$, and in its vicinity the dispersion is well approximated by

$$(1 - \omega/\omega_e) \approx \eta_e (1 - k/k_e)^6 \quad (5)$$

where $k_e = \pi/d$ is the 6DBE wavenumber at the band edge. In analogy to the theory presented in [10], the dimensionless ‘‘flatness parameter’’ η_e is related to the value of the sixth

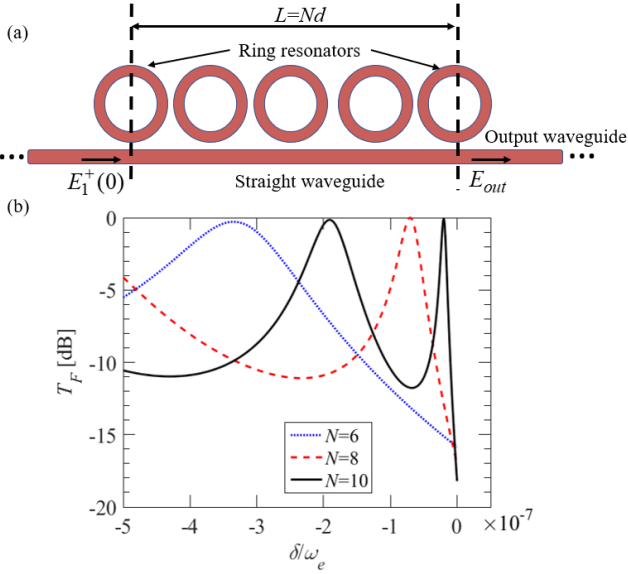


Fig. 3. (a) Finite length 6DBE-CROW of length $L=Nd$, where N is the number of unit cells. The straight waveguide is extended on both sides working as input and output waveguide. The 6DBE-CROW is excited from the left extended waveguide by the field amplitude $E_1^+(0)$ and the output electric field amplitude exiting the waveguide from the right is E_{out} . (b) Magnitude of the transfer function T_F in dB of a 6DBE-CROW operating in close proximity of the 6DBE frequency calculated for three different number of unit cells (N) of the 6DBE-CROW given as 6, 8 and 10. Resonances of such a cavity, denoted by transmission peaks, gets sharper when they get closer to the 6DBE frequency, i.e., when $\delta = \omega - \omega_e \rightarrow 0$. The longer the cavity, the closer the resonances to the 6DBE frequency.

derivative of ω with respect to k at the 6DBE angular frequency ω_e , i.e.,

$$d^6 \omega / dk^6 = -\eta_e \omega_e / (720k_e^6) \quad (6)$$

and it dictates the flatness of the dispersion relation at ω_e . Such fitting formula is shown with red cross markers in Fig. 2(a) with the flatness parameter $\eta_e = 0.00025$. The flatness parameter plays an important role in the scaling of the quality factor of the whole structure as explained in [10].

IV. Giant Resonance in CROW with Sixth Order EPD

We start this section by showing the transfer function of a cavity made of a lossless finite-length 6DBE-CROW, as shown in Fig. 3(a), for different numbers of unit cells. We recall that a unit cell is made of two rings, since the coupling coefficients are alternating from one ring to its adjacent one, as shown in Fig. 1. A unit cell starts at the center of the ring just before the coupling point with the straight waveguide, as shown with a dashed line in Fig. 3(a). At each end there are three ports to be terminated. The first and last rings are terminated with half rings; whereas the straight waveguide is extended to define the input and output, without changing the waveguide dimensions. The transfer function is defined as

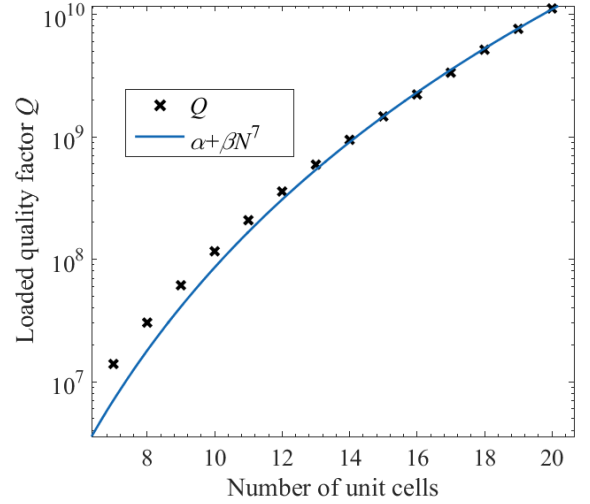


Fig. 4. Loaded quality factor (Q) of the lossless 6DBE-CROW calculated at different cavity lengths, i.e., for growing number of unit cells N . The values of Q , denoted by black cross symbols, are calculated using the group delay method while the blue solid line represents the fitting curve with equation $Q = \alpha + \beta N^7$.

$$T_F = \left| \frac{E_{out}}{E_1^+(0)} \right| \quad (7)$$

where E_{out} is the electric field wave amplitude escaping the straight output waveguide from the right, while $E_1^+(0)$ is the incident-wave field amplitude to the waveguide from the left. A cavity has multiple resonances as shown in Fig. 3(b), and the resonance frequency closest to the 6DBE frequency, denoted by $\omega_{r,e}$ (the closest transmission peak), exhibits the narrowest spectral width, as seen for the case of $N=10$ unit cells in Fig. 3(b). Also, one can see that the 6DBE resonance gets sharper (higher Q factor) and it gets closer to ω_e by increasing the number of unit cells N of a cavity. Such trend for the 6DBE resonance frequency follows the asymptotic formula

$$\omega_{r,e} / \omega_e \approx 1 - \eta_e / N^6 \quad (8)$$

in analogy to what was discussed in [5], [10] for a fourth order degeneracy.

Now, we analyze the scaling of the Q factor with the length of a 6DBE-CROW cavity where the straight waveguide continues without terminations or discontinuities on both left and right ends of the waveguide, as shown in Fig. 3(a). The loaded Q factor of the cavity versus the number of unit cells N is shown in Fig. 4, where the Q factor is calculated through the group delay as was done in [4], [9], [10]. The scaling of the Q factor versus N is fitted by $\alpha + \beta N^7$ where the fitting parameters α and β for the case shown in Fig. 4 are given as $\alpha \approx 27.3$ and $\beta \approx 8.5$. Hence, we show here that the 6DBE-CROW cavity made of a waveguide structure of finite length has a Q factor that asymptotically grows with length as

$$Q \approx \beta N^7. \quad (9)$$

V. Applications of 6DBE-CROWs Operating Near a 6DBE

We show two possible applications associated with the finite-length 6DBE-CROW operating near the 6DBE: an ultra-low-threshold laser and an ultra-sensitive sensor.

A. Low threshold optical oscillator

In this section we explore an interesting application of the 6DBE-CROW which is a low threshold oscillator. To investigate the lasing threshold in a finite 6DBE-CROW, we introduce distributed gain only in the ring resonators of a finite lossless 6DBE-CROW. The distributed gain may be introduced by doping the rings or their surrounding with optically pumped active atoms, e.g., Er^{3+} , or by using layers of quantum wells [32]. Here we model the distributed gain as a negative imaginary part of the effective refractive index of the ring resonators, i.e., $n_r = n_{\text{real}} + i n_{\text{imag}}$, where in the introduced design $n_{\text{real}} = 2.45$ and n_{imag} is dictated by the concentration of the active material and the pumping power. Hence, we define the per unit length propagation power gain as $\gamma = -2k_0 n_{\text{imag}}$ [m^{-1}], where k_0 is the free space wavenumber [9] (also see Ch.5, P. 229 in [33]). Note that if we introduce large gain into the 6DBE-CROW, this would deteriorate the degeneracy and the unique properties associated with the slow-wave phenomena, as discussed in [32], [34]. So, we start with small values of distributed gain and increase it gradually, monitoring when the structure starts oscillating. This is done by tracking the complex frequency poles loci of the transfer function T_F [35] when varying the distributed propagation gain values. Hence, we calculate the lasing gain threshold γ_{th} defined as the minimum amount of distributed propagation gain (assumed uniform along the structure) that is sufficient to maintain lasing in the 6DBE-CROW cavity through stimulated emission. In Fig. 5 we show the scaling of the lasing threshold versus number of unit cells N constituting the finite-length 6DBE-CROW, which is shown with black markers. The extraordinary property of the 6DBE-CROW is that the lasing threshold decreases with increasing number of unit cells N , i.e., increasing the structure length, following the unique trend

$$\gamma_{th} \approx p N^{-7} \quad (10)$$

where p is a fitting constant, as shown with the dashed black fitting curve in Fig. 5. This result is quite expected as the scaling of the oscillation threshold is inversely proportional to the scaling of the quality factor [9], that in turn is proportional to N^7 as discussed in Sec. IV.

In order to demonstrate the advantage of the 6th order EPD over the lower EPD orders, we compare the lasing threshold of the CROW operating near a 6DBE with another CROW of the same length, but different coupling parameters, that is operating near a DBE (4th order EPD) at the same frequency [9], [30]. The threshold in the DBE case is denoted by blue markers in Fig. 5,

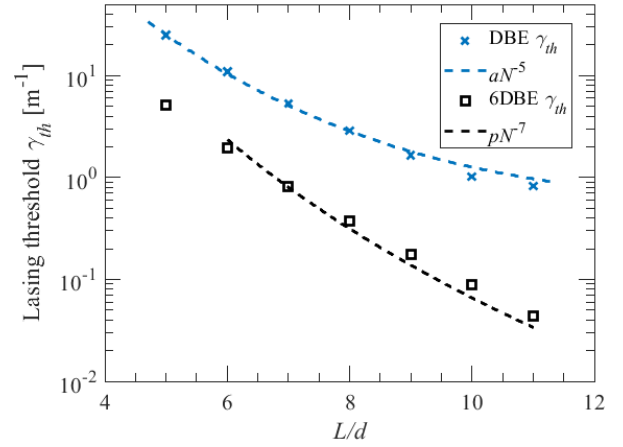


Fig. 5. Lasing threshold of a finite-length 6DBE-CROW calculated for different lengths of the structure. Blue markers represent the calculated threshold for a cavity operating near the DBE (4th order EPD) whereas black markers are the calculated threshold for a cavity operating near the 6DBE. Dashed lines represent the fitting of these data: the blue one represents the scaling $\gamma_{th,DBE} = aN^{-5}$ of the DBE laser [32], whereas the black one represents the asymptotic scaling $\gamma_{th,6DBE} = pN^{-7}$ of a 6DBE laser.

where the fitting curve of the lasing threshold scaling $\gamma_{th,DBE} \propto aN^{-5}$ with N is shown with blue dashed line. It is clear that the 6DBE provides lower lasing threshold than the DBE and a stronger scaling with the CROW length, representing a new scaling law for lasing threshold.

B. Ultra-sensitive optical sensor

Another interesting property of EPDs is that they are very sensitive to perturbations that make them very promising for sensor applications [19], [36]. This also poses strict constraints on fabrication tolerances as already discussed in [10] referring to the 4th order DBE. In order to demonstrate this sensitivity property, we consider the eigenvalues and dispersion relation of the infinite periodic circuit around the 6DBE condition. The tiny physical perturbation of the waveguide (in frequency, refractive index, couplings, losses, dimensions, etc) is modeled by a tiny perturbation ϵ of the transfer matrix $\underline{\mathbf{T}}$ as $\underline{\mathbf{T}} = \underline{\mathbf{T}}_e + \epsilon \underline{\mathbf{T}}'$, where $\underline{\mathbf{T}}_e$ is the transfer matrix generating the 6DBE and $\underline{\mathbf{T}}'$ accounts for the perturbed terms. In close proximity of the 6DBE, the perturbed eigenvalues of the system characterized by the perturbed transfer matrix $\underline{\mathbf{T}}$ are obtained using the Puiseux series expansion [37], [38] around the ideal degenerate eigenvalue ζ_e , which is approximated to the first order as

$$\zeta_q(\epsilon) \approx \zeta_e + \alpha_1 e^{iq\pi/3} \epsilon^{1/6} \quad (11)$$

for $q = 1, 2, 3, \dots, 6$, where $\zeta_e = \pm 1$ is the 6DBE degenerate eigenvalue, ϵ is the perturbation factor of any parameter from the designed 6DBE value, and the Puiseux series coefficient α_1 is calculated using the formula provided in [38]. It is worth

mentioning that α_1 depends on both the perturbed system parameter and the flatness of the 6DBE. Since $\zeta_q = \exp(ik_q d)$ and $\zeta_e = \exp(ik_e d)$, the Puiseux series for the eigenvalues ζ_q leads to the following first order approximation fractional power expansion of the six Bloch wavenumbers in the vicinity of the 6DBE wavenumber $k_e = 0$ or $k_e = \pi/d$:

$$k_q(\epsilon) \approx k_e - i\alpha_1 d^{-1} e^{-ik_e d} e^{iq\pi/3} \epsilon^{1/6} \quad (12)$$

This equation shows that there are 6 different perturbed Bloch wavenumber, and the perturbations $k_q(\epsilon) - k_e$ are proportional to $\epsilon^{1/6}$ which means the wavenumber shows much higher sensitivity for small values of the perturbation ϵ than the linear proportionality in a regular straight waveguide. Further investigation of the 6DBE sensitivity is beyond the scope of this paper and it can be a subject for future studies including system tolerances and other perturbing effects. We just add that in the case where ϵ represents a perturbation to the operating 6DBE angular frequency, i.e., $\epsilon = (\omega - \omega_e)/\omega_e$, the relation between α_1 and the flatness parameter η_e in (5) is $\alpha_1 = k_e d (\eta_e)^{-1/6}$. In the case of $k_e = 0$, η_e in (5) would also vanish; hence α_1 would assume a finite value.

Finally, we would like to point out that in this paper we only considered lossless structures. Some effect of losses and structural perturbations of the CROW were discussed before in [4], [10]; however such analysis was presented for the DBE case and more studies in this direction shall be performed. Losses are expected to have a larger impact in the case of the 6DBE than the DBE case. Furthermore, it is expected that the impact of losses is also affected by the flatness constant η_e in (5). This higher sensitivity to losses and other perturbations may be disadvantageous for some applications, but at the same time it definitely represents an outstanding advantage in several applications like optical sensors, modulators and optical switches.

Conclusion

We used a periodic CROW to show for the first time a possible realization of a 6th order exceptional point of degeneracy at optical frequencies. We have investigated the quality factor of a cavity made of a finite-length CROW resonating near the 6DBE frequency and we have shown that the scaling of the loaded Q factor of the 6DBE-CROW is proportional to N^7 for lossless CROWs. Finally, we have shown two possible applications of the 6DBE-CROW: low threshold lasers where the lasing threshold was found to scale with the CROW length as $g_{th} \propto N^{-7}$ when the CROW operates near the 6DBE. Moreover, we have shown the perturbation of the CROW eigenvalues near a 6DBE due to a small structural perturbation δ and it was shown that it is proportional to $\delta^{1/6}$ indicating how a 6DBE-CROW is very sensitive to small perturbations.

Acknowledgment

This material is based on work supported by the Air Force Office of Scientific Research award number FA9550-15-1-0280 and by the National Science Foundation under award NSF ECCS-171197.

References

- [1] C. M. Bender, "Making sense of non-Hermitian Hamiltonians," *Rep. Prog. Phys.*, vol. 70, no. 6, p. 947, 2007.
- [2] C. E. Rüter, K. G. Makris, R. El-Ganainy, D. N. Christodoulides, M. Segev, and D. Kip, "Observation of parity-time symmetry in optics," *Nat. Phys.*, vol. 6, no. 3, pp. 192–195, 2010.
- [3] A. Figotin and I. Vitebskiy, "Electromagnetic unidirectionality in magnetic photonic crystals," *Phys. Rev. B*, vol. 67, no. 16, p. 165210, 2003.
- [4] M. Y. Nada, M. A. K. Othman, and F. Capolino, "Theory of coupled resonator optical waveguides exhibiting high-order exceptional points of degeneracy," *Phys. Rev. B*, vol. 96, no. 18, p. 184304, Nov. 2017.
- [5] A. Figotin and I. Vitebskiy, "Gigantic transmission band-edge resonance in periodic stacks of anisotropic layers," *Phys. Rev. E*, vol. 72, no. 3, p. 0036619, 2005.
- [6] A. Figotin and I. Vitebskiy, "Slow wave phenomena in photonic crystals," *Laser Photonics Rev.*, vol. 5, no. 2, pp. 201–213, Mar. 2011.
- [7] N. Gutman, C. Martijn de Sterke, A. A. Sukhorukov, and L. C. Botten, "Slow and frozen light in optical waveguides with multiple gratings: Degenerate band edges and stationary inflection points," *Phys. Rev. A*, vol. 85, no. 3, p. 033804, Mar. 2012.
- [8] J. R. Burr, N. Gutman, C. M. de Sterke, I. Vitebskiy, and R. M. Reano, "Degenerate band edge resonances in coupled periodic silicon optical waveguides," *Opt. Express*, vol. 21, no. 7, pp. 8736–8745, Apr. 2013.
- [9] M. A. K. Othman, F. Yazdi, A. Figotin, and F. Capolino, "Giant gain enhancement in photonic crystals with a degenerate band edge," *Phys. Rev. B*, vol. 93, no. 2, p. 024301, Jan. 2016.
- [10] M. Y. Nada, M. A. K. Othman, O. Boyraz, and F. Capolino, "Giant Resonance and Anomalous Quality Factor Scaling in Degenerate Band Edge Coupled Resonator Optical Waveguides," *J. Light. Technol.*, vol. 36, no. 14, pp. 3030–3039, Jul. 2018.
- [11] J. Scheuer, G. T. Paloczi, J. K. S. Poon, and A. Yariv, "Coupled Resonator Optical Waveguides: Toward the Slowing and Storage of Light," *Opt. Photonics News*, vol. 16, no. 2, p. 36, Feb. 2005.
- [12] H. Altug and J. Vučković, "Experimental demonstration of the slow group velocity of light in two-dimensional coupled photonic crystal microcavity arrays," *Appl. Phys. Lett.*, vol. 86, no. 11, p. 111102, Mar. 2005.
- [13] M. Soljacic and J. D. Joannopoulos, "Enhancement of nonlinear effects using photonic crystals," *Nat. Mater.*, vol. 3, no. 4, pp. 211–219, Apr. 2004.
- [14] K. Sakoda, "Enhanced light amplification due to group-velocity anomaly peculiar to two- and three-dimensional photonic crystals," *Opt. Express*, vol. 4, no. 5, p. 167, Mar. 1999.
- [15] A. Figotin and I. Vitebskiy, "Slow light in photonic crystals," *Waves Random Complex Media*, vol. 16, no. 3, pp. 293–382, Aug. 2006.
- [16] H. Kazemi, M. Y. Nada, T. Mealy, A. F. Abdelshafy, and F. Capolino, "Exceptional Points of Degeneracy Induced by Linear Time-Periodic Variation," *Phys. Rev. Appl.*, vol. 11, no. 1, p. 014007, Jan. 2019.
- [17] A. F. Abdelshafy, M. A. K. Othman, D. Oshmarin, A. T. Almutawa, and F. Capolino, "Exceptional Points of Degeneracy in Periodic Coupled Waveguides and the Interplay of Gain and Radiation Loss: Theoretical and Experimental Demonstration," *IEEE Trans. Antennas Propag.*, pp. 1–1, 2019.
- [18] W. Bernard, G. Geister, and M. Raab, "Optical ring resonator sensor," US5305087 A, 19-Apr-1994.
- [19] J. Wiersig, "Enhancing the Sensitivity of Frequency and Energy Splitting Detection by Using Exceptional Points: Application to Microcavity Sensors for Single-Particle Detection," *Phys. Rev. Lett.*, vol. 112, no. 20, p. 203901, May 2014.
- [20] C. Peng, Z. Li, and A. Xu, "Rotation sensing based on a slow-light resonating structure with high group dispersion," *Appl. Opt.*, vol. 46, no. 19, p. 4125, 2007.
- [21] K. J. Vahala, "Optical microcavities," *Nature*, vol. 424, no. 6950, pp. 839–846, Aug. 2003.

- [22] C. Zou, J. Cui, F. Sun, X. Xiong, X. Zou, Z. Han, and G. Guo, "Guiding light through optical bound states in the continuum for ultrahigh-Q microresonators," *Laser Photonics Rev.*, vol. 9, no. 1, pp. 114–119, Jan. 2015.
- [23] Z. Qiang, W. Zhou, and R. A. Soref, "Optical add-drop filters based on photonic crystal ring resonators," *Opt. Express*, vol. 15, no. 4, pp. 1823–1831, Feb. 2007.
- [24] J. E. Heebner and R. W. Boyd, "Enhanced all-optical switching by use of a nonlinear fiber ring resonator," *Opt. Lett.*, vol. 24, no. 12, p. 847, Jun. 1999.
- [25] J. K. S. Poon, J. Scheuer, Y. Xu, and A. Yariv, "Designing coupled-resonator optical waveguide delay lines," *J. Opt. Soc. Am. B*, vol. 21, no. 9, p. 1665, Sep. 2004.
- [26] S. L. McCall, A. F. J. Levi, R. E. Slusher, S. J. Pearton, and R. A. Logan, "Whispering-gallery mode microdisk lasers," *Appl. Phys. Lett.*, vol. 60, no. 3, pp. 289–291, Jan. 1992.
- [27] A. Yariv, Y. Xu, R. K. Lee, and A. Scherer, "Coupled-resonator optical waveguide: proposal and analysis," *Opt. Lett.*, vol. 24, no. 11, p. 711, Jun. 1999.
- [28] H. Ramezani, S. Kalish, I. Vitebskiy, and T. Kottos, "Unidirectional Lasing Emerging from Frozen Light in Nonreciprocal Cavities," *Phys. Rev. Lett.*, vol. 112, no. 4, p. 043904, Jan. 2014.
- [29] R. Almhadi and K. Sertel, "Frozen-Light Modes in 3-way Coupled Silicon Ridge Waveguides," in *2019 United States National Committee of URSI National Radio Science Meeting (USNC-URSI NRSRM)*, Boulder, CO, USA, 9-12 Jan. 2019, pp. 1–2.
- [30] M. A. K. Othman, M. Veysi, A. Figotin, and F. Capolino, "Low Starting Electron Beam Current in Degenerate Band Edge Oscillators," *IEEE Trans. Plasma Sci.*, vol. 44, no. 6, pp. 918–929, Jun. 2016.
- [31] H. Haus, W. Huang, S. Kawakami, and N. Whitaker, "Coupled-mode theory of optical waveguides," *J. Light. Technol.*, vol. 5, no. 1, pp. 16–23, Jan. 1987.
- [32] M. Veysi, M. A. K. Othman, A. Figotin, and F. Capolino, "Degenerate band edge laser," *Phys. Rev. B*, vol. 97, no. 19, p. 195107, May 2018.
- [33] A. Yariv and P. Yeh, *Photonics: Optical Electronics in Modern Communications (The Oxford Series in Electrical and Computer Engineering)*. Oxford University Press, Inc., New York 2007.
- [34] J. Grgić, J. R. Ott, F. Wang, O. Sigmund, A. Jauho, J. Mork, and N. A. Mortensen, "Fundamental Limitations to Gain Enhancement in Periodic Media and Waveguides," *Phys. Rev. Lett.*, vol. 108, no. 18, p. 183903, May 2012.
- [35] G. F. Franklin, J. D. Powell, A. Emami-Naeini, and J. D. Powell, *Feedback control of dynamic systems*, vol. 3. Addison-Wesley Reading, MA, 1994.
- [36] W. Chen, S. Kaya Özdemir, G. Zhao, J. Wiersig, and L. Yang, "Exceptional points enhance sensing in an optical microcavity," *Nature*, vol. 548, no. 7666, pp. 192–196, Aug. 2017.
- [37] T. Kato, *Perturbation theory for linear operators*, vol. 132. Springer, 1995.
- [38] A. Welters, "On explicit recursive formulas in the spectral perturbation analysis of a Jordan block," *SIAM J. Matrix Anal. Appl.*, vol. 32, no. 1, pp. 1–22, 2011.